

Protein Kinase A-mediated Phosphorylation of Pah1p Phosphatidate Phosphatase Functions in Conjunction with the Pho85p-Pho80p and Cdc28p-Cyclin B Kinases to Regulate Lipid Synthesis in Yeast*

Received for publication, July 18, 2012, and in revised form, July 31, 2012. Published, JBC Papers in Press, August 3, 2012, DOI 10.1074/jbc.M112.402339

Wen-Min Su, Gil-Soo Han, Jessica Casciano, and George M. Carman¹

From the Department of Food Science and Rutgers Center for Lipid Research, Rutgers University, New Brunswick, New Jersey 08901

Background: Pah1p, a phosphatidate phosphatase in yeast, produces diacylglycerol for lipid synthesis.

Results: Phosphorylation of Pah1p by protein kinase A inhibited membrane association, phosphatidate phosphatase activity, and triacylglycerol synthesis.

Conclusion: Protein kinase A functioned in conjunction with Pho85p-Pho80p and Cdc28p-cyclin B kinases to regulate Pah1p.

Significance: Lipid synthesis is regulated through multiple phosphorylations of Pah1p phosphatidate phosphatase.

Pah1p, which functions as phosphatidate phosphatase (PAP) in the yeast *Saccharomyces cerevisiae*, plays a crucial role in lipid homeostasis by controlling the relative proportions of its substrate phosphatidate and its product diacylglycerol. The diacylglycerol produced by PAP is used for the synthesis of triacylglycerol as well as for the synthesis of phospholipids via the Kennedy pathway. Pah1p is a highly phosphorylated protein *in vivo* and has been previously shown to be phosphorylated by the protein kinases Pho85p-Pho80p and Cdc28p-cyclin B. In this work, we showed that Pah1p was a *bona fide* substrate for protein kinase A, and we identified by mass spectrometry and mutagenesis that Ser-10, Ser-677, Ser-773, Ser-774, and Ser-788 were the target sites of phosphorylation. Protein kinase A-mediated phosphorylation of Pah1p inhibited its PAP activity by decreasing catalytic efficiency, and the inhibitory effect was primarily conferred by phosphorylation at Ser-10. Analysis of the S10A and S10D mutations (mimicking dephosphorylation and phosphorylation, respectively), alone or in combination with the seven alanine (7A) mutations of the sites phosphorylated by Pho85p-Pho80p and Cdc28p-cyclin B, indicated that phosphorylation at Ser-10 stabilized Pah1p abundance and inhibited its association with membranes, PAP activity, and triacylglycerol synthesis. The S10A mutation enhanced the physiological effects imparted by the 7A mutations, whereas the S10D mutations attenuated the effects of the 7A mutations. These data indicated that the protein kinase A-mediated phosphorylation of Ser-10 functions in conjunction with the phosphorylations mediated by Pho85p-Pho80p and Cdc28p-cyclin B and that phospho-Ser-10 should be dephosphorylated for proper PAP function.

PAP,² which was first identified in animal tissues by Kennedy and co-workers (1), has emerged as a key enzyme in lipid metabolism that has a significant impact on obesity, lipodystrophy, and the metabolic syndrome (2–5). The enzyme catalyzes the Mg²⁺-dependent dephosphorylation of PA to yield DAG and P_i (Fig. 1) (1). The DAG generated in the reaction is used to synthesize TAG, as well as the major phospholipids PC and phosphatidylethanolamine (6–8). PA is also used for the synthesis of phospholipids via the liponucleotide intermediate CDP-DAG (6, 7), and PAP activity has a negative regulatory effect on *de novo* phospholipid synthesis (9). Thus, PAP being positioned at the PA branch point plays an important role in lipid synthesis (6–8).

The yeast *Saccharomyces cerevisiae* serves as an excellent model in elucidating the enzymological, kinetic, and regulatory properties of PAP (9–14). The *PAH1* gene in *S. cerevisiae* was first identified to encode PAP (9), and this discovery led to the identifications of homologous PAP-encoding genes in humans (9, 15), mice (16, 17), flies (18, 19), worms (20), and plants (21, 22). All PAP orthologs³ have in common the haloacid dehalogenase-like domain that contains a DXDX(T/V) catalytic motif and the NLIP domain found at the N terminus whose function is unclear (Fig. 1) (4, 9, 16, 23). Mutations of the conserved aspartate residues in the catalytic motif eliminate PAP activity and its physiological functions (23).

A phenotypic characterization of yeast mutants defective in Pah1p PAP activity has revealed the importance of the enzyme in lipid metabolism and cell physiology. The *pah1Δ* mutant, which has reduced levels of DAG and increased levels of PA,

* This work was supported, in whole or in part, by National Institutes of Health Grant GM-50679 from the USPHS.

¹ To whom correspondence should be addressed: Dept. of Food Science, Rutgers University, 65 Dudley Rd., New Brunswick, NJ 08901. Tel.: 848-932-5407; E-mail: carman@aesop.rutgers.edu.

² The abbreviations used are: PAP, phosphatidate phosphatase; PA, phosphatidate; DAG, diacylglycerol; TAG, triacylglycerol; ER, endoplasmic reticulum; 4A/4D, alanine/aspartate mutations of Ser-677, Ser-773, Ser-774, Ser-788; 5A/5D, alanine/aspartate mutations of Ser-10, Ser-677, Ser-773, Ser-774, Ser-788; 7A, alanine mutations of Ser-110, Ser-114, Ser-168, Ser-602, Thr-723, Ser-744 and Ser-748.

³ The PAP orthologs in various organisms are known by different acronyms that are based on the names of genes that encode the enzyme. For example, in *S. cerevisiae*, the protein product of the *PAH1* gene is known as Pah1p (9), whereas in human and mouse, the protein products of the *LPIN1* and *Lpin1* genes, respectively, are known as lipin 1 (16).

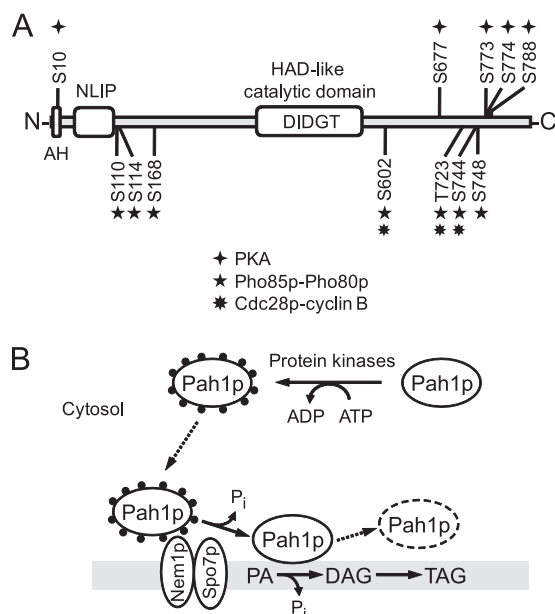


FIGURE 1. Pah1p sites phosphorylated by PKA, Pho85p-Pho80p, and Cdc28p-cyclin B and model for the regulation by phosphorylation/dephosphorylation. *A*, domain structure of Pah1p showing the positions of the amphipathic helix (AH), NLIP domain, the haloacid dehalogenase (HAD)-like domain containing the DIDGT catalytic motif, and the serine (S) and threonine (T) residues that are phosphorylated by PKA (this study), Pho85p-Pho80p (32), and Cdc28p-cyclin B (29). *B*, Pah1p in the cytosol is phosphorylated on sites (black circles decorating Pah1p) by multiple protein kinases. The phosphorylated enzyme is translocated to the nuclear/ER membrane (dotted arrow) for its dephosphorylation by the Nem1p-Spo7p phosphatase complex. The dephosphorylated membrane-associated form of Pah1p catalyzes the dephosphorylation of PA to generate DAG for the synthesis of TAG. The dotted line ellipse signifies the loss of Pah1p after catalysis (32).

exhibits a great reduction in TAG and a significant increase in phospholipid content (9, 23, 24). Elevated PA content also correlates with the induced expression of UAS_{INO}-containing phospholipid synthesis genes (due to loss of Opi1p repressor function) and the aberrant expansion of the nuclear/ER membrane (9, 23–25). Reduced DAG content correlates with defects in lipid droplet formation (26) and vacuole homeostasis and fusion (27). The reduced ability to synthesize TAG renders PAP mutants acutely sensitive to fatty acid-induced toxicity (24). In addition, loss of Pah1p causes a respiratory deficiency phenotype and sensitivity to growth at elevated temperature (9, 25). Elevated Pah1p PAP activity is also deleterious to lipid homeostasis and cell physiology. For example, the overexpression of an unregulated form of PAP inhibits cell growth, and this can be attributed to the depletion of PA needed for phospholipid synthesis via CDP-DAG and to the accumulation of DAG to a toxic level (28–30). Because an excess as well as loss of PAP activity is detrimental to cell physiology, the enzyme should be fine-tuned to control lipid metabolism. Although PAP is regulated by nucleotides (e.g. inhibition by ATP and CTP) (13) and sphingoid bases (e.g. inhibition by phytosphingosine and sphinganine) (12), the major mechanism for its regulation is through phosphorylation/dephosphorylation (28, 29, 31, 32).

Pah1p is a peripheral membrane enzyme, and its membrane association is governed by its state of phosphorylation (29, 31, 32). Pah1p is found in the cytosol as a phosphoprotein, which is recruited to the nuclear/ER membrane and dephosphorylated

by the Nem1p-Spo7p phosphatase complex (Fig. 1) (25, 29, 31, 33). The dephosphorylation allows Pah1p to directly associate with the membrane via a short N-terminal amphipathic helix for interaction with its substrate PA and enzyme catalysis (31). The inhibitory effect of phosphorylation on PAP activity and direct membrane association is mediated by multiple protein kinases (34). Proteome-wide phosphorylation studies have shown that Pah1p is phosphorylated by the cyclin-dependent protein kinases Pho85p (35, 36) and Cdc28p (37). These proline-directed Ser/Thr protein kinases are known to play roles in cell cycle progression, gene expression, macromolecular metabolism, and signaling in response to environmental conditions (38–40). Pho85p-Pho80p protein kinase-cyclin complex phosphorylates Pah1p on six serine residues and one threonine residue (Fig. 1) (32). These phosphorylations inhibit PAP activity, prevent its interaction with the membrane, and inhibit the synthesis of TAG (32). Three of the sites phosphorylated by Pho85p-Pho80p are also phosphorylated by the Cdc28p-cyclin B complex (Fig. 1), but individually these phosphorylations have little effect on PAP function (29). Collectively, however, the phosphorylations of the seven Ser/Thr-Pro sites play a major role in controlling the enzyme's function in lipid metabolism (28, 29, 32).

In addition to the cyclin-dependent protein kinases, Pah1p is also phosphorylated by PKA (41). PKA is the principal mediator of signals transmitted through the RAS/cAMP pathway in *S. cerevisiae*, and it plays a role in controlling cell metabolism, including phospholipid synthesis (42–44). Herein, we identify the PKA phosphorylation sites in Pah1p (Fig. 1). Using phosphorylation-deficient mutant enzymes, we show that phosphorylation of Ser-10, alone and in combination with the seven sites phosphorylated by Pho85p-Pho80p and Cdc28p-cyclin B, attenuated Pah1p PAP function in lipid synthesis.

EXPERIMENTAL PROCEDURES

Materials—Growth medium supplies were obtained from Difco. Qiagen was the supplier of the DNA gel extraction kit, plasmid DNA purification kit, and nickel-nitilotriacetic acid-agarose resin. The QuikChange site-directed mutagenesis kit, carrier DNA for yeast transformation, and enzyme reagents for DNA manipulations were obtained from Stratagene, Clontech, and New England Biolabs, respectively. PCR primers were prepared by Genosys Biotechnologies. DNA size ladders, molecular mass protein standards, and reagents for electrophoresis, Western blotting, and protein determination were purchased from Bio-Rad. IgG-Sepharose, PVDF paper, and the enhanced chemifluorescence Western blotting detection kit were from GE Healthcare. PKA catalytic subunit (bovine heart) was from Promega. Lipids and thin layer chromatography plates (cellulose and silica gel 60) were from Avanti Polar Lipids and EM Science, respectively. Radiochemicals were from PerkinElmer Life Sciences, and scintillation counting supplies and acrylamide solutions were from National Diagnostics. Alkaline phosphatase-conjugated goat anti-rabbit IgG antibodies, alkaline phosphatase-conjugated goat anti-mouse IgG antibodies, mouse anti-phosphoglycerate kinase antibodies, and rabbit anti-(phosphoserine/phosphothreonine) PKA substrate antibodies were from Thermo Scientific, Pierce, Invitrogen, and

Phosphorylation of Yeast Phosphatidate Phosphatase

TABLE 1
Strains used in this work

Strain	Relevant characteristics	Source or Ref
<i>E. coli</i>		
DH5 α	F ⁻ ϕ 80 <i>lacZ</i> Δ M15 Δ (<i>lacZYA-argF</i>)U169 <i>deoR recA1 endA1 hsdR17</i> (<i>r_k⁻ m_k⁺</i>) <i>phoA supE44</i> I ⁻ <i>thi-1 gyrA96 relA1</i>	49
BL21(DE3)pLysS	F ⁻ <i>ompT hsdS_B</i> (<i>r_B⁻ m_B⁻</i>) <i>gal dcm</i> (DE3) pLysS	Novagen
<i>S. cerevisiae</i>		
RS453	<i>MATa ade2-1 his3-11,15 leu2-3,112 trp1-1 ura3-52</i>	84
SS1026	<i>pah1</i> Δ :: <i>TRP1</i> derivative of RS453	25
SS1132	<i>pah1</i> Δ :: <i>TRP1 nem1</i> Δ :: <i>HIS3</i> derivative of RS453	29

Cell Signaling Technology, respectively. Bovine serum albumin, phosphoamino acid standards, L-1-tosylamido-2-phenylethyl chloromethyl ketone-trypsin, protease inhibitors, and Triton X-100 were purchased from Sigma. All other chemicals were reagent grade or better.

Strains and Growth Conditions—Table 1 lists the *Escherichia coli* and *S. cerevisiae* strains used in this work. *E. coli* strains DH5 α and BL21(DE3)pLysS were used for the propagation of plasmids and for the expression of yeast His₆-tagged Pah1p, respectively. The bacterial cells were grown at 37 °C in LB medium (1% tryptone, 0.5% yeast extract, 1% NaCl (pH 7)). For the selection of cells carrying plasmids for the expression of Pah1p, the growth medium was supplemented with ampicillin (100 μ g/ml) and chloramphenicol (34 μ g/ml) (45). The expression of Pah1p in cells bearing *PAH1* derivatives of plasmid pET-15b was induced with 1 mM isopropyl β -D-thiogalactoside (9). *S. cerevisiae* strains SS1026 and SS1132 are *pah1* Δ and *pah1* Δ *nem1* Δ mutants, respectively, and were used for the expression of wild type and phosphorylation-deficient forms of Pah1p. Yeast cells were grown in standard synthetic complete medium containing 2% glucose, and appropriate amino acids were omitted from the growth medium to select for cells carrying specific plasmids (46). Synthetic complete growth medium lacking inositol and choline was prepared as described by Culbertson and Henry (47). Growth of cultures (200 μ l) in 96-well plates was monitored with a Thermomax plate reader. The modified Gompertz equation (48) was used to calculate growth parameters. Cell numbers in liquid cultures were determined spectrophotometrically at an absorbance of 600 nm. The liquid growth medium was supplemented with agar (2% for yeast or 1.5% for *E. coli*) for growth on solid medium.

DNA Manipulations—Isolation of genomic and plasmid DNA, digestion and ligation of DNA, and PCR amplification of DNA were performed by standard protocols (49, 50). The plasmids used in this study are listed in Table 2. Plasmid pGH313 directs the isopropyl β -D-1-thiogalactopyranoside-induced expression of His₆-tagged Pah1p in *E. coli* (9), whereas plasmid pGH315 directs low copy expression of Pah1p in *S. cerevisiae* (29). pGH313-1-752 and pGH313-1-646 were constructed by generating a nonsense mutation at codon 753 and codon 647, respectively, of pGH313. pGH313-18-862 was constructed from pGH313 by replacing codons 1-17 with a start codon, and pGH313-235-752 was produced from pGH313-235-862 by replacing codons 753-862 with a stop codon. The derivatives of pGH313 and pGH315 that contain serine-to-alanine/aspartate mutations were constructed by QuikChange site-directed mutagenesis using appropriate templates and primers. Plasmids containing multiple missense mutations were constructed

by the general strategies described previously (29). All mutations were confirmed by DNA sequencing. Plasmid transformations of *E. coli* (49) and yeast (51) were performed as described previously.

Purification of Pah1p—His₆-tagged wild type and mutant forms of Pah1p expressed in *E. coli* BL21(DE3)pLysS were purified by affinity chromatography using nickel-nitrilotriacetic acid-agarose (9, 45). Pah1p was also purified from *S. cerevisiae* as described by O'Hara *et al.* (28).

Preparation of Yeast Cell Extracts and Subcellular Fractionation—All steps were performed at 4 °C. Yeast cell extracts were prepared by disruption of cells with glass beads (0.5 mm diameter) using a BioSpec Products Mini-BeadBeater-16 (52). The cell disruption buffer contained 50 mM Tris-HCl (pH 7.5), 0.3 M sucrose, 0.15 M NaCl, 10 mM 2-mercaptoethanol, 0.5 mM phenylmethanesulfonyl fluoride, 1 mM benzamidine, 5 μ g/ml aprotinin, 5 μ g/ml leupeptin, and 5 μ g/ml pepstatin (9). The cytosol (supernatant) and total membrane (pellet) fractions were separated by centrifugation at 100,000 \times *g* for 1 h (52). The membrane pellets were suspended in the cell disruption buffer to the same volume of the cytosol fraction. Protein concentration was estimated by the method of Bradford (53) using bovine serum albumin as the standard.

Phosphorylation of Pah1p by PKA—Phosphorylation reactions were performed in triplicate for 10 min at 30 °C in a total volume of 20 μ l. The standard reaction mixture contained 25 mM Tris-HCl (pH 7.5), 10 mM MgCl₂, 2 mM dithiothreitol, 100 μ M [γ -³²P]ATP (3,000 cpm/pmol), Pah1p (50 μ g/ml), and the indicated amounts of PKA. At the end of the phosphorylation reactions, samples were subjected to SDS-PAGE (54). A unit of PKA activity was defined as the amount of enzyme that catalyzed the formation of 1 nmol of phosphorylated product/min.

Mass Spectrometry Analysis of Pah1p Phosphorylation Sites—Mass spectrometry analysis of phosphorylated Pah1p was performed at the Center for Advanced Proteomics Research of the University of Medicine and Dentistry of New Jersey, Newark. After trypsin digestion of phosphorylated Pah1p in SDS-polyacrylamide gel slices, peptides were analyzed by matrix-assisted laser desorption ionization tandem time-of-flight mass spectrometry to identify phosphopeptide candidates. Based on the phosphopeptide ion inclusion list, quadrupole time-of-flight and Orbitrap liquid chromatography-mass spectrometry/mass spectrometry were performed to identify phosphorylation sites (29).

Phosphoamino Acid and Phosphopeptide Mapping Analyses—Phosphorylated (*i.e.* ³²P-labeled) Pah1p resolved in the SDS-polyacrylamide gel was transferred to a PVDF membrane and was subjected to acid hydrolysis with 6 N HCl at 110 °C (for

TABLE 2
Plasmids used in this work

Plasmid	Relevant characteristics	Source or Ref
pET-15b	<i>E. coli</i> expression vector with N-terminal His ₆ tag fusion	Novagen
pGH313	<i>PAH1</i> coding sequence inserted into pET-15b	9
pGH313-1-752	<i>PAH1</i> (1-752 truncation) derivative of pGH313	This study
pGH313-1-646	<i>PAH1</i> (1-646 truncation) derivative of pGH313	This study
pGH313-235-752	<i>PAH1</i> (235-752 truncation) derivative of pGH313	This study
pGH313-18-862	<i>PAH1</i> (18-862 truncation) derivative of pGH313	This study
pGH313-S10A	<i>PAH1</i> (S10A) derivative of pGH313	This study
pGH313-S677A	<i>PAH1</i> (S677A) derivative of pGH313	This study
pGH313-S773A	<i>PAH1</i> (S773A) derivative of pGH313	This study
pGH313-S774A	<i>PAH1</i> (S774A) derivative of pGH313	This study
pGH313-S773A/S774A	<i>PAH1</i> (S773A/S774A) derivative of pGH313	This study
pGH313-S788A	<i>PAH1</i> (S788A) derivative of pGH313	This study
pGH313-5A	<i>PAH1</i> (S10A/S677A/S773A/S774A/S788A) derivative of pGH313	This study
pRS415	Low copy <i>E. coli</i> /yeast shuttle vector with <i>LEU2</i>	85
pGH315	<i>PAH1</i> inserted into pRS415	29
pGH315-S10A	<i>PAH1</i> (S10A) derivative of pGH315	This study
pGH315-S10D	<i>PAH1</i> (S10D) derivative of pGH315	This study
pGH315-S677A	<i>PAH1</i> (S677A) derivative of pGH315	This study
pGH315-S677D	<i>PAH1</i> (S677D) derivative of pGH315	This study
pGH315-S773A	<i>PAH1</i> (S773A) derivative of pGH315	This study
pGH315-S773D	<i>PAH1</i> (S773D) derivative of pGH315	This study
pGH315-S774A	<i>PAH1</i> (S774A) derivative of pGH315	This study
pGH315-S774D	<i>PAH1</i> (S774D) derivative of pGH315	This study
pGH315-S788A	<i>PAH1</i> (S788A) derivative of pGH315	This study
pGH315-S788D	<i>PAH1</i> (S788D) derivative of pGH315	This study
pGH315-4A	<i>PAH1</i> (S677A/S773A/S774A/S788A) derivative of pGH315	This study
pGH315-4D	<i>PAH1</i> (S677D/S773D/S774D/S788D) derivative of pGH315	This study
pGH315-5A	<i>PAH1</i> (S10A/S677A/S773A/S774A/S788A) derivative of pGH315	This study
pGH315-5D	<i>PAH1</i> (S10D/S677D/S773D/S774D/S788D) derivative of pGH315	This study
pGH315-7A	<i>PAH1</i> (S110A/S114A/S168A/S602A/T723A/S744A/S748A) derivative of pGH315	29
pGH315-S10A-7A	<i>PAH1</i> (S10A/S110A/S114A/S168A/S602A/T723A/S744A/S748A) derivative of pGH315	This study
pGH315-S10D-7A	<i>PAH1</i> (S10D/S110A/S114A/S168A/S602A/T723A/S744A/S748A) derivative of pGH315	This study

phosphoamino acid analysis) or to proteolytic digestion with L-1-tosylamido-2-phenylethyl chloromethyl ketone-trypsin (for phosphopeptide mapping analysis) (55–57). Acid hydrolysates of Pah1p were mixed with standard phosphoamino acids and separated by two-dimensional electrophoresis on cellulose thin layer chromatography plates, whereas tryptic digests of Pah1p were separated by electrophoresis and TLC using cellulose thin layer chromatography plates (55–57). Radioactive phosphoamino acids and phosphopeptides were visualized by phosphorimaging analysis, and standard phosphoamino acids were visualized with ninhydrin stain.

SDS-PAGE and Western Blot Analysis—SDS-PAGE (54) and Western blotting (58, 59) with PVDF membrane were performed by standard protocols. Rabbit anti-Pah1p antibodies (29), rabbit anti-phosphatidylserine synthase antibodies (60), and mouse anti-phosphoglycerate kinase antibodies were used at a concentration of 2 µg/ml. Rabbit anti-(phosphoserine/phosphothreonine) PKA substrate antibodies were used at a dilution of 1:1,000. Alkaline phosphatase-conjugated goat anti-rabbit IgG antibodies and goat anti-mouse IgG antibodies were used at a dilution of 1:5,000. Immune complexes were detected using the enhanced chemifluorescence Western blotting detection kit. Fluorimaging was used to acquire images from Western blots, and the relative densities of the images were analyzed using ImageQuant software. Signals were in the linear range of detectability.

Measurement of PAP Activity—PAP activity was measured by following the release of water-soluble ³²P_i from chloroform-soluble [³²P]PA (10,000 cpm/nmol) (52). The ³²P-labeled PA used for the assay was enzymatically synthesized from DAG and [γ-³²P]ATP using *E. coli* DAG kinase (52). The reaction contained 50 mM Tris-HCl (pH 7.5), 1 mM MgCl₂, 0.2 mM PA, 2

mM Triton X-100, and enzyme protein in a total volume of 0.1 ml. All enzyme assays were conducted in triplicate at 30 °C. The average standard deviation of the assays was ±5%. The reactions were linear with time and protein concentration. A unit of PAP activity was defined as the amount of enzyme that catalyzed the formation of 1 nmol of product per min.

Labeling and Analysis of Lipids—Steady-state labeling of lipids with [2-¹⁴C]acetate was performed as described previously (61), and lipids were extracted from labeled cells by the method of Bligh and Dyer (62). Lipids were analyzed by one-dimensional thin layer chromatography on silica gel plates (63). The identity of radiolabeled TAG and total phospholipids on TLC plates was confirmed by comparison of its migration with that of standards after exposure to iodine vapor. Radiolabeled lipids were visualized by phosphorimaging analysis and were quantified using ImageQuant software.

Analyses of Data—Statistical analyses were performed with SigmaPlot software. The *p* values <0.05 were taken as a significant difference. The enzyme kinetics module of SigmaPlot software was used to analyze kinetic data according to the Michaelis-Menten and Hill equations.

RESULTS

PKA Phosphorylates Pah1p and Attenuates Its PAP Activity—The phosphorylation of Pah1p with PKA was characterized using purified recombinant Pah1p and pure PKA catalytic subunit from bovine heart. By using Pah1p expressed in *E. coli*, we eliminated any prior phosphorylations that occur when the enzyme is expressed in yeast (28). The mammalian protein kinase is structurally and functionally similar to the *S. cerevisiae* PKA catalytic subunit (64) and thus has been used to study the phosphorylation of several phospholipid synthesis proteins

Phosphorylation of Yeast Phosphatidate Phosphatase

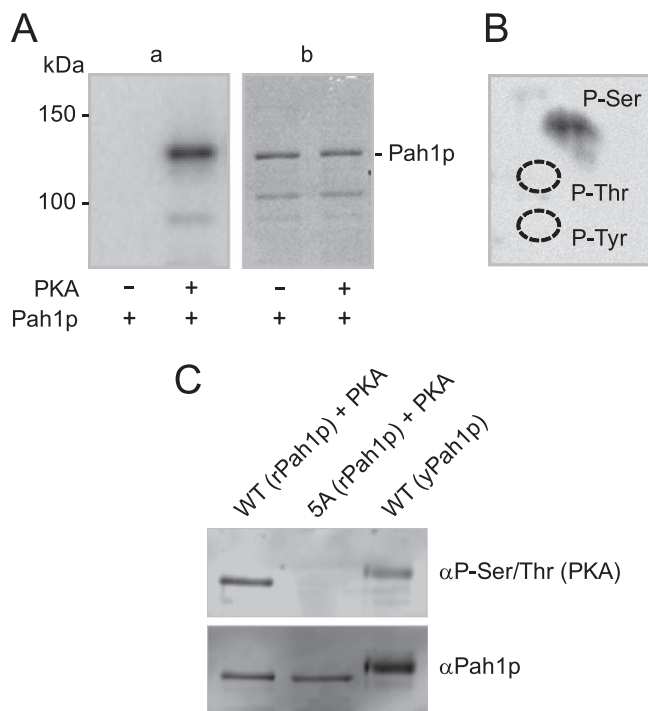


FIGURE 2. PKA phosphorylates Pah1p on a serine residue *in vitro* and *in vivo*. *A*, purified recombinant Pah1p (1 μ g) was phosphorylated with PKA (2 units) and [γ - 32 P]ATP (1 nmol) for 10 min. Following the reaction, Pah1p was separated from ATP and PKA by SDS-PAGE. The polyacrylamide gel was dried and subjected to phosphorimaging analysis (*panel a*). After the imaging analysis, the dried gel was swollen with water and stained with Coomassie Blue (*panel b*). The positions of molecular mass standards and Pah1p are indicated. *B*, PVDF membrane containing 32 P-labeled Pah1p was incubated with 6 N HCl for 90 min at 110 $^{\circ}$ C, and the hydrolysates were separated by two-dimensional electrophoresis. The positions of the standard phosphoamino acids phosphoserine (P-Ser), phosphothreonine (P-Thr) (dotted lines), and phosphotyrosine (P-Tyr) (dotted lines) are indicated in the figure. *C*, samples (1 μ g) of wild type Pah1p purified from *S. cerevisiae* (yPah1p) and purified recombinant (rPah1p) wild type and 5A mutant enzymes that were incubated with PKA (20 units) and ATP (1 nmol) for 20 min were subjected to SDS-PAGE and Western blot analysis using anti-(phosphoserine/phosphothreonine) PKA substrate antibodies (α P-Ser/Thr (PKA)). The membranes were stripped and then re-probed with anti-Pah1p antibodies (α Pah1p). The data shown in A–C are representative of three experiments.

from yeast (60, 65–67). The *in vitro* phosphorylation was measured by following the incorporation of the radioactive phosphate of [γ - 32 P]ATP into Pah1p (Fig. 2A). The position of the phosphorylated Pah1p on SDS-polyacrylamide gels was confirmed by Coomassie Blue staining of the protein on the gel (Fig. 2A). PKA is a serine/threonine-specific protein kinase (68), and phosphoamino acid analysis indicated that the enzyme phosphorylates Pah1p only on a serine residue (Fig. 2B).

Previous studies have shown that Pah1p isolated from *S. cerevisiae* is a phosphoprotein (28). We sought evidence that some of this phosphorylation was mediated by PKA. To address this question, we made use of antibodies that are generated against a peptide containing phosphoserine/phosphothreonine within the PKA consensus motif (Cell Signaling Technology). Indeed, these antibodies recognized Pah1p isolated from yeast (Fig. 2C), which had been known to be phosphorylated *in vivo* on Ser-773 and Ser-774 (28). These are two of the five sites that were found here to be targets of PKA *in vitro* (see below). To confirm that these antibodies recognized Pah1p phosphorylated by PKA, a Western blot was performed on purified recom-

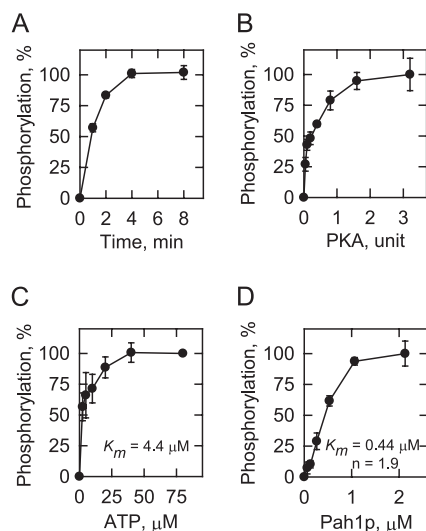


FIGURE 3. Pah1p is a *bona fide* substrate of PKA. Phosphorylation of Pah1p by PKA was measured by following the incorporation of the radiolabeled phosphate from [γ - 32 P]ATP into purified recombinant Pah1p under standard reaction conditions by varying time (*A*), the amount of PKA (*B*), the ATP concentration (*C*), and the Pah1p concentration (*D*). Following the phosphorylation reactions, the samples were subjected to SDS-PAGE; the polyacrylamide gels were dried and then subjected to phosphorimaging analysis. The relative amounts of phosphate incorporated into Pah1p were quantified using ImageQuant software. The data shown in A–D are the averages of three experiments \pm S.D. (error bars).

binant wild type and 5A mutant (see below) enzymes that were incubated with PKA and ATP. The antibodies recognized wild type Pah1p phosphorylated with PKA but did not recognize the PKA-treated 5A mutant enzyme (Fig. 2C). The electrophoretic mobility of the Pah1p isolated from yeast was slower than the enzyme isolated from *E. coli* (Fig. 2C). This was due to the fact that in yeast Pah1p is phosphorylated by Pho85p-Pho80p and Cdc28p-cyclin B at Thr-723, an event that also causes a decrease in the electrophoretic mobility of the purified recombinant enzyme (32).

PKA activity was further characterized to confirm that Pah1p was a *bona fide* substrate. The phosphorylation was dependent on the time of the reaction (Fig. 3A) and the amount of PKA used in the reaction (Fig. 3B). In addition, the dependences of PKA activity on ATP and Pah1p followed saturation kinetics (Fig. 3C) and positive cooperative kinetics (Fig. 3D), respectively. The analysis of the kinetic data indicated that K_m values for ATP and Pah1p were 4.4 and 0.44 μ M, respectively, and a Hill number for Pah1p was 1.9. At the point of maximum phosphorylation (Fig. 3), PKA catalyzed the incorporation of 1 mol of phosphate/mol of Pah1p.

To examine the effect of PKA phosphorylation on PAP activity, the phosphorylated and unphosphorylated forms of Pah1p were assayed for enzyme dependence on the surface concentration of PA. The surface concentration of PA, as opposed to its molar concentration, was varied because PAP activity follows surface dilution kinetics (9, 11, 69). Under the conditions of these experiments, PAP activity was independent of the molar concentration of PA (11). As described previously (9), the unphosphorylated enzyme showed positive cooperative (Hill number of 2.4) kinetics with respect to PA (Fig. 4A). The PKA phosphorylation of Pah1p caused a decrease in PAP activity

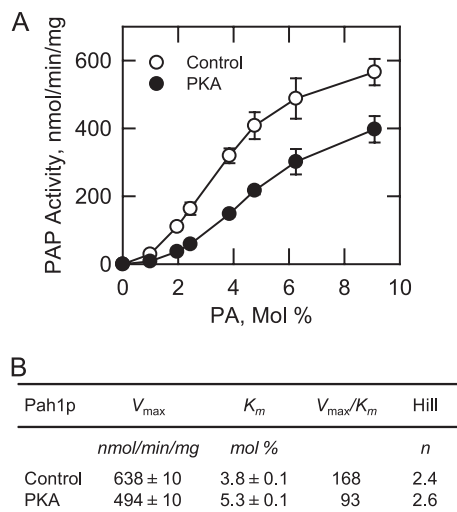


FIGURE 4. Phosphorylation of Pah1p by PKA attenuates PAP activity. A, purified recombinant Pah1p (0.5 μ g) was incubated with and without PKA (PKA, 20 units) and ATP (1 nmol) for 5 min. The PAP activity of the phosphorylated and unphosphorylated forms of the enzyme was measured as a function of the surface concentration (mol %) of PA. The molar concentration of PA was held constant at 0.2 mM, and the molar concentration of Triton X-100 was varied to obtain the indicated surface concentrations. The values indicated were the average of three experiments \pm S.D. (error bars). B, V_{max} , K_m , and Hill values were determined from the data in A using the Enzyme Kinetics module of SigmaPlot software.

(Fig. 4A) with a reduction in V_{max} and an increase in K_m values (Fig. 4B). Consequently, the phosphorylation of Pah1p by PKA caused a 1.8-fold decrease in its catalytic efficiency (Fig. 4B). The phosphorylation, however, did not affect the cooperative behavior of PAP activity.

Ser-10, Ser-677, Ser-773, Ser-774, and Ser-788 in Pah1p Are Phosphorylated by PKA—A combination of mass spectrometry and mutagenesis was used to identify PKA phosphorylation sites in Pah1p. In an initial approach, full-length and truncated forms of recombinant Pah1p were phosphorylated with PKA and [γ - 32 P]ATP and were subjected to phosphopeptide mapping analysis. The phosphopeptide map of full-length Pah1p showed multiple signals, indicating that PKA phosphorylated Pah1p at several sites (Fig. 5B, WT). Analyses of the phosphopeptide maps derived from truncations at the N- and C-terminal ends of Pah1p indicated that one site is between amino acid residues 1 and 18 and the remaining sites are between amino acid residues 646 and 862 (Fig. 5B).

The mass spectrometry analysis of peptides from the phosphorylated full-length protein identified Ser-773, Ser-774, and Ser-788 as phosphorylation sites. To confirm these sites, Pah1p with alanine mutations were expressed in *E. coli*, purified, phosphorylated with PKA, and subjected to phosphopeptide mapping analysis. Each of the three mutations (e.g. S773A, S774A, and S788A) affected the phosphopeptide map of Pah1p, and by comparing the maps of the wild type and mutant proteins, we could assign which sites were contained within the phosphopeptides present in the map of wild type Pah1p (Fig. 5C). Four phosphopeptides could be attributed to Ser-773 and Ser-774, and the S773A/S774A double mutation eliminated the four phosphopeptides from the map. The maps of the individual mutations indicated that Ser-773 was the more heavily phosphorylated when compared with Ser-774. That

multiple spots in the phosphopeptide map contained the same phosphorylation sites indicated incomplete proteolytic digestions.

Analysis of the full-length N- and C-terminal truncations and the S773A, S774A, and S788A mutants revealed there were additional sites that had not been identified by mass spectrometry. The unidentified sites were located between amino acid 1 and 18 and between 646 and 752 (Fig. 5B). There are four serine residues (e.g. Ser-10, Ser-12, Ser-16, and Ser-17) between amino acids 1 and 18, none of which is contained within a PKA consensus sequence, whereas the 646–752 region contains three putative PKA sites (Ser-677, Ser-692, and Ser-694). Alanine mutations of the seven residues were constructed, expressed in *E. coli*, and subjected to phosphopeptide mapping after phosphorylation with PKA. The only mutations that affected the phosphorylation of Pah1p were S10A and S677A. The phosphopeptides that contained Ser-10 and Ser-677 (Fig. 5B, WT) were missing in the phosphopeptide maps of the S10A and S677A mutant enzymes (Fig. 5C).

The effects of each of the PKA phosphorylation site mutations on Pah1p phosphorylation and activity are shown in Fig. 6. Each of the five single mutations caused a reduction in phosphorylation by 50–66%, whereas the quintuple mutation (e.g. 5A mutation) abolished the phosphorylations by PKA (Fig. 6A). The 5A mutation also eliminated the inhibitory effect that PKA had on PAP activity, and this effect was primarily attributed to the S10A mutation (Fig. 6B).

Phosphorylation State of Ser-10 Alone and in Combination with the 7A Mutations Affects Cell Growth—Serine-to-alanine/aspartate mutations were constructed for the five PKA phosphorylation sites to examine the physiological effects of phosphorylation deficiency/mimicry of Pah1p. The mutant proteins were expressed in both *pah1* Δ *NEM1* and *pah1* Δ *nem1* Δ mutant cells. In this way, we could examine the dependence of Pah1p function on Nem1p-Spo7p protein phosphatase activity. In addition, the expression of the phosphorylation site mutants in *nem1* Δ affords examination of the mutations in a genetic background that favors phosphorylation of other nonmutated phosphorylation sites in Pah1p.

The *pah1* Δ mutant exhibits a temperature-sensitive phenotype (e.g. loss of growth at 37 $^{\circ}$ C) that reflects an important role of PAP activity in lipid metabolism (9, 23, 70). The expression of wild type *PAH1* in the *pah1* Δ mutant allowed some growth on agar plates at 37 $^{\circ}$ C, but the growth was more limited in the *nem1* Δ mutant background (Fig. 7) (29). This emphasized the importance of Nem1p-Spo7p phosphatase activity for normal PAP function *in vivo* (29). The expression of *PAH1* with the five alanine mutations alone and in combination did not have a major effect on the complementation of the *pah1* Δ temperature-sensitive phenotype regardless of whether or not *NEM1* was present (Fig. 7). The five aspartate mutations did not affect the complementation of temperature sensitivity when *NEM1* was present (Fig. 7A). However, in the *nem1* Δ mutant background, the S10D and 5D mutations did not permit growth on agar plates at 37 $^{\circ}$ C (Fig. 7B). The other four aspartate mutations alone and in combination were not distinguished from wild type *PAH1* with respect to the complementation of growth

Phosphorylation of Yeast Phosphatidate Phosphatase

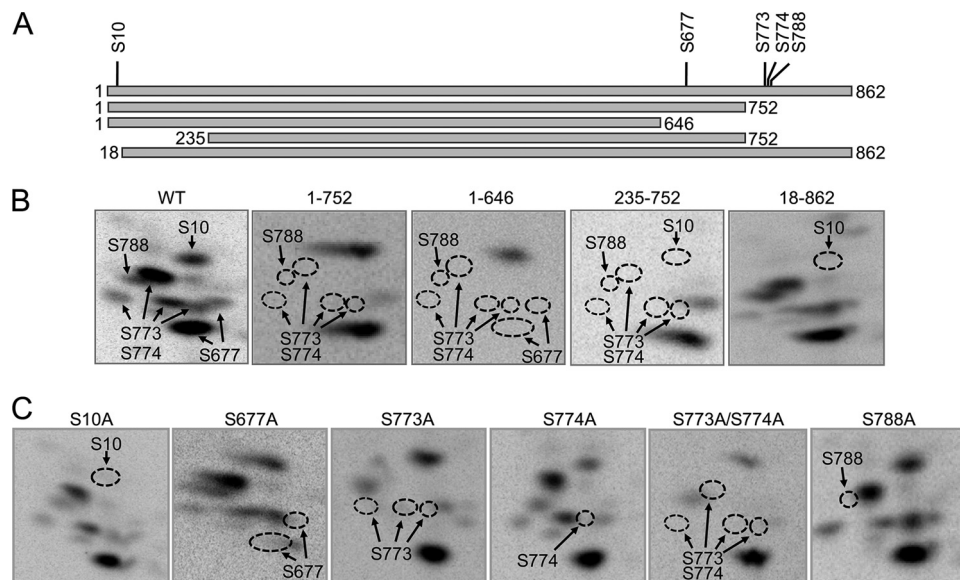


FIGURE 5. Phosphopeptide mapping analysis of Pah1p mutants phosphorylated by PKA. *A*, diagrams show the full-length and truncated versions of *E. coli*-expressed recombinant Pah1p that were used for phosphorylation and phosphopeptide mapping analysis. The positions of the Pah1p phosphorylation sites are indicated in the full-length protein. Purified recombinant WT and the indicated truncation (*B*) and phosphorylation site (*C*) Pah1p mutants (1 μ g) were phosphorylated with PKA (20 units) and [γ - 32 P]ATP (2 nmol) for 20 min. After phosphorylation, the samples were subjected to SDS-PAGE and transferred to PVDF membrane. The 32 P-labeled proteins were digested with L-1-tosylamido-2-phenylethyl chloromethyl ketone-trypsin. The resulting peptides were separated on cellulose thin layer plates by electrophoresis (from left to right) in the first dimension and by chromatography (from bottom to top) in the second dimension. The identity of the phosphorylation sites in the radioactive phosphopeptides of the wild type enzyme was determined from the maps of the Pah1p mutant enzymes. The positions of the phosphopeptides that were absent in the mutant enzymes (indicated by the dotted line ellipse) but were present in the wild type enzyme are indicated in the figure. The data are representative of three independent experiments.

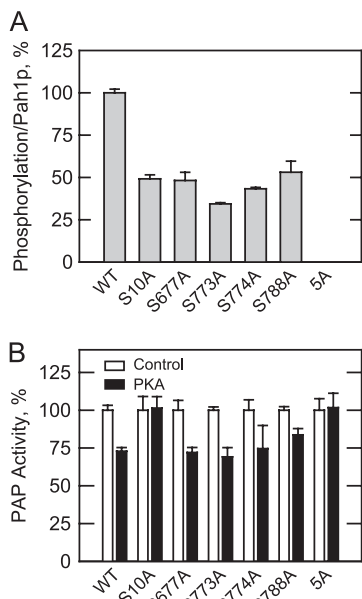


FIGURE 6. Effects of PKA phosphorylation site mutations on the phosphorylation of Pah1p and on the inhibitory effects of PKA on PAP activity. WT and the indicated phosphorylation site mutant Pah1p enzymes were expressed and purified from *E. coli*. *A*, recombinant Pah1p (50 μ g/ml) was phosphorylated with PKA (40 units) and [γ - 32 P]ATP (50 μ M) for 20 min. Following the reaction, Pah1p was separated from ATP and PKA by SDS-PAGE. The polyacrylamide gel was dried and subjected to phosphorimaging and ImageQuant analysis. Afterward, the dried gel was swollen with water, stained with Coomassie Blue, and subjected to image analysis. The relative phosphorylation/Pah1p of the mutant enzymes was compared with the wild type enzyme that was set at 100%. The data reported are the average of three independent experiments \pm S.D. (error bars). *B*, recombinant wild type and mutant Pah1p enzymes were phosphorylated with PKA and then assayed for PAP activity under standard assay conditions. The controls for the mutant enzymes were the unphosphorylated mutant forms of the enzyme. The values reported were the average of three experiments \pm S.D. (error bars).

at 37 $^{\circ}$ C (Fig. 7*B*). Thus, the lack of growth caused by the 5D mutations was attributed to the S10D mutation.

These results suggested that Nem1p-Spo7p dephosphorylates other sites to compensate for the loss of Pah1p function caused by the S10D mutation. Previous studies have shown that phosphorylation of Pah1p by Pho85p-Pho80p and Cdc28p-cyclin B on seven Ser/Thr-Pro sites is a major regulator of PAP function (32, 71). Moreover, the expression of *PAH1* with alanine mutations of the seven sites (7*A*) allowed for growth of *pah1* Δ *nem1* Δ mutant cells on agar plates at 37 $^{\circ}$ C (Fig. 8*B*), indicating that the 7*A* mutations can bypass the requirement of Nem1p-Spo7p for Pah1p PAP function (29, 31). Thus, we decided to investigate the effects of mutations in Ser-10 in combination with the 7*A* mutations. When S10A + 7*A* mutations were expressed in *pah1* Δ and *pah1* Δ *nem1* Δ cells, the growth on agar plates at 37 $^{\circ}$ C was attenuated when compared with the growth of cells expressing the 7*A* mutations alone (Fig. 7). In fact, the growth of cells carrying these mutations appeared less at the permissive temperature of 30 $^{\circ}$ C (Fig. 7). Accordingly, growth was examined in more detail in liquid medium at 30 $^{\circ}$ C (Fig. 8). In the presence and absence of *NEM1*, the growth of cells expressing the S10A + 7*A* mutations was reduced when compared with cells expressing wild type *PAH1* and *PAH1* with the S10A, S10D, S10D + 7*A*, and 7*A* mutations. The S10A + 7*A* mutations caused increases in both the lag time (*pah1* Δ *NEM1*, from 5.9 \pm 0.1 to 9.9 \pm 0.1 h; *pah1* Δ *nem1* Δ , from 6.6 \pm 0.1 to 9.5 \pm 0.1 h) and the generation time (*pah1* Δ *NEM1*, from 4.8 \pm 0.2 to 6.0 \pm 0.1 h; *pah1* Δ *nem1* Δ , from 4.4 \pm 0.2 to 5.4 \pm 0.1 h) when compared with wild type *PAH1*. However, by the time cells reached the stationary phase, the cell density of cells expressing the S10A + 7*A* mutations was not significantly dif-

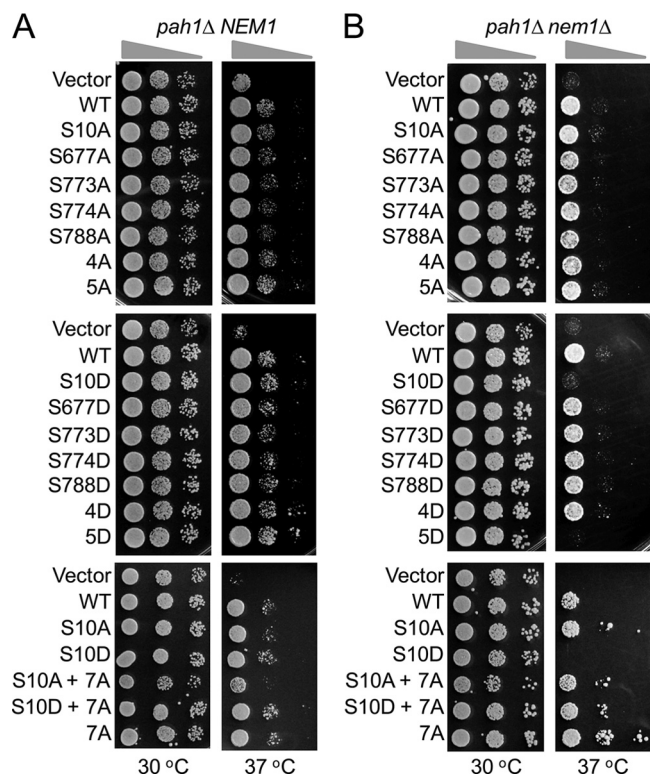


FIGURE 7. Effects of PKA phosphorylation site mutations on the complementation of the *pah1Δ* temperature-sensitive phenotype. The indicated wild type and phosphorylation site mutant forms of *PAH1* were expressed in *pah1Δ NEM1* (A) and *pah1Δ nem1Δ* (B) cells. Serial dilutions (10-fold) of the cells were then spotted onto agar plates and were incubated at 30 and 37 °C for 3–4 days. The data are representative of three independent experiments.

ferent from the wild type control (Fig. 8). This result indicated that the mutations affected Pah1p function during the exponential phase of growth.

We questioned if the growth defects caused by the S10A + 7A mutations at 30 °C could be overcome by supplementations with inositol and choline. We reasoned that if these mutations gave rise to a more active PAP enzyme, then PA would be channeled into DAG and TAG at the expense of phospholipid synthesis via the CDP-DAG pathway (72, 73). At the same time, a reduction in PA levels would cause the translocation of the repressor *Opilp* into the nucleus where it would inhibit the expression of *INO1* (a key gene encoding an enzyme for inositol synthesis) and other UAS_{INO} -containing phospholipid synthesis genes (72, 73). Thus, the combination of inositol and choline would bypass the repression of *INO1* and stimulate the synthesis of phosphatidylinositol and PC (via the Kennedy pathway) (44, 73). In fact, the addition of inositol and choline did correct the slower growth caused by the S10A + 7A mutations (Fig. 8).

Phosphorylation State of Ser-10 in Combination with the 7A Mutations Affect the Abundance and the Localization of Pah1p—The Pah1p levels of the phosphorylation site mutant enzymes expressed in *pah1Δ NEM1* and in *pah1Δ nem1Δ* cells were examined by Western blot analysis using anti-Pah1p antibodies. This analysis indicated that none of the serine-to-alanine/aspartate mutations had a major effect on the abundance of Pah1p (data not shown). As described previously (32, 71), the 7A mutations caused a decrease (30% in *pah1Δ NEM1* and 45% in *pah1Δ nem1Δ*) in Pah1p abundance (Fig. 9). The S10A muta-

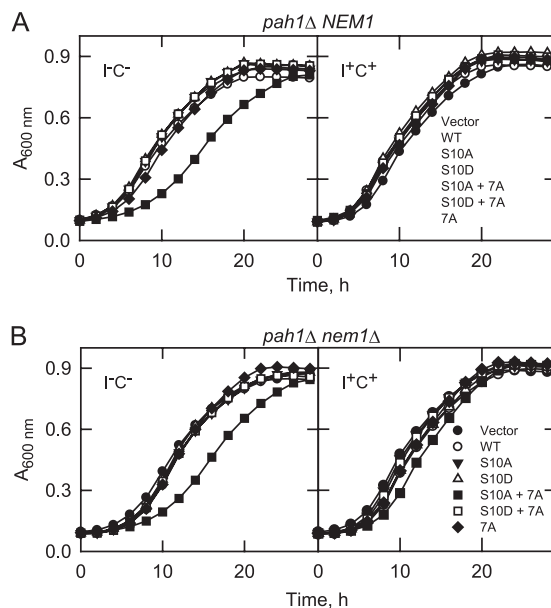


FIGURE 8. S10A mutation in combination with the 7A mutations reduces growth in medium lacking inositol and choline. The indicated wild type and phosphorylation site mutant forms of *PAH1* were expressed in *pah1Δ NEM1* (A) and *pah1Δ nem1Δ* (B) cells. Cells were grown in synthetic medium without (I^-C^-) and with inositol and choline (I^+C^+). Growth was monitored at $A_{600\text{ nm}}$. Each data point represents the average of three independent cultures, and the average S.D. for each data point was $\pm 3\%$.

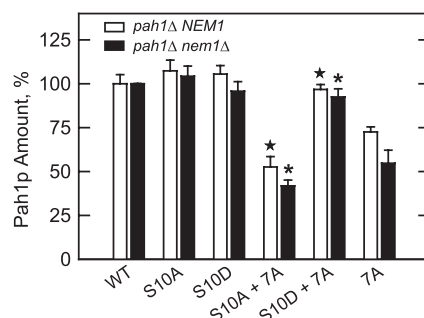


FIGURE 9. Phosphorylation state of Ser-10 in combination with the 7A mutations affect the abundance of Pah1p. The indicated wild type and phosphorylation site mutant forms of *PAH1* were expressed in *pah1Δ NEM1* and *pah1Δ nem1Δ* cells. Cell extracts prepared from exponential phase cells were subjected to Western blot analysis using anti-Pah1p and anti-phosphoglycerate kinase antibodies. The relative amounts of Pah1p from the cells were determined by ImageQuant analysis of the data. Each data point represents the average of four experiments \pm S.D. (error bars). *, $p < 0.05$ versus 7A in *pah1Δ NEM1*; *, $p < 0.05$ versus 7A in *pah1Δ nem1Δ*.

tion in combination with 7A caused a further reduction (28 and 25%, respectively) in Pah1p abundance. Conversely, Pah1p abundance in *pah1Δ NEM1* and *pah1Δ nem1Δ* cells expressing the S10D + 7A mutations was similar to that observed for wild type Pah1p expressed in these cells (Fig. 9). These data indicated that the S10D mutation had a stabilizing effect on the loss of abundance caused by the 7A mutations, whereas the S10A mutation enhanced the destabilizing effect of the 7A mutations.

The effects of the PKA phosphorylation site mutations on the localization of Pah1p were examined. In *pah1Δ NEM1* and *pah1Δ nem1Δ* cells, greater than 90% of wild type Pah1p was associated with the cytosolic fraction. This amount is slightly greater than that shown in our previous work (29, 32). This may be explained by the fact that in this study we included 0.15 M

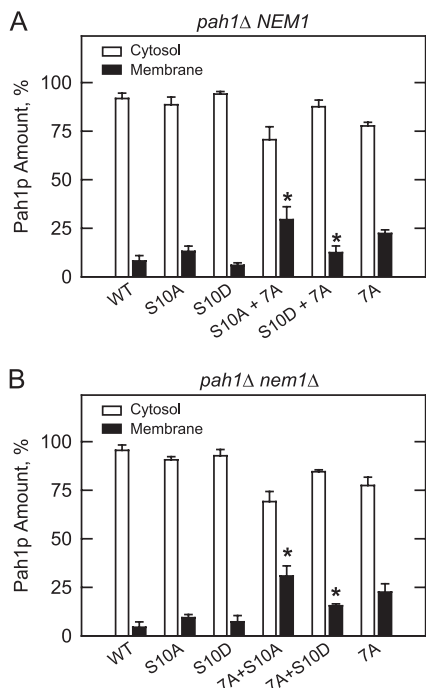


FIGURE 10. Phosphorylation state of Ser-10 in combination with the 7A mutations affect the localization of Pah1p. The indicated wild type and phosphorylation site mutant forms of *PAH1* were expressed in *pah1Δ NEM1* (A) and *pah1Δ nem1Δ* (B) cells. Cell extracts prepared from exponential phase cells were fractionated into the cytosol and membrane fractions by centrifugation. The membrane fraction was resuspended in the same volume as the cytosol fraction, and equal volumes of the fractions were subjected to Western blot analysis using anti-Pah1p, anti-phosphoglycerate kinase (cytosol marker), and anti-phosphatidylserine synthase (ER marker) antibodies. The Western blot analysis for the marker proteins indicated highly enriched cytosol and membrane fractions as described previously (71). The relative amounts of cytosol and membrane-associated Pah1p were determined for the wild and phosphorylation site mutant forms of the enzyme by ImageQuant analysis of the data. Each data point represents the average of four experiments \pm S.D. (error bars). *, $p < 0.05$ versus 7A membrane.

NaCl in the buffers to prevent nonspecific associations of Pah1p with membranes. None of the single mutations had a significant effect on the localization of Pah1p whether they were expressed in *pah1Δ NEM1* or *pah1Δ nem1Δ* cells. Consistent with our previous work (29, 32), the 7A mutations caused an increase (175% in *pah1Δ NEM1* and 411% in *pah1Δ nem1Δ*) in the association of Pah1p with membranes (Fig. 10). In combination with the 7A mutations, S10A caused a further increase (32% in *pah1Δ NEM1* and 37% in *pah1Δ nem1Δ*) in membrane association. However, the amounts of Pah1p associated with membranes of *pah1Δ NEM1* and *pah1Δ nem1Δ* cells expressing the S10D + 7A mutations were 45 and 33% less, respectively, when compared with the cells expressing the 7A mutations (Fig. 10).

Phosphorylation State of Ser-10 in Combination with the 7A Mutations Affect TAG Content—The effects of the PKA phosphorylation site mutations on the amounts of TAG were examined. Our analysis was performed at the stationary phase because this is the phase of growth where the effect of PAP on TAG content is most pronounced (9, 23, 24). As described previously (29), the TAG content of *pah1Δ nem1Δ* cells expressing wild type *PAH1* was reduced by 5.8-fold when compared with *pah1Δ NEM1* cells expressing the wild type gene (Fig. 11A). The reduction of TAG content in *pah1Δ nem1Δ* cells expressing

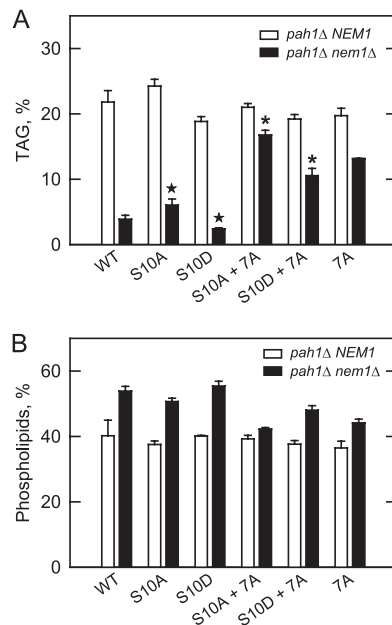


FIGURE 11. Phosphorylation state of Ser-10 in combination with the 7A mutations affects lipid content. The indicated wild type and phosphorylation site mutant forms of *PAH1* were expressed in *pah1Δ NEM1* and *pah1Δ nem1Δ* cells. Cultures were grown to the stationary phase in synthetic medium containing [2-¹⁴C]acetate (1 μ Ci/ml). Lipids were extracted and separated by one-dimensional TLC, and the phosphorimages were subjected to ImageQuant analysis. The percentages shown for TAG (A) and phospholipids (B) were normalized to the total ¹⁴C-labeled chloroform-soluble fraction. Each data point represents the average of three experiments \pm S.D. (error bars). *, $p < 0.05$ versus WT in *pah1Δ nem1Δ*; *, $p < 0.05$ versus 7A in *pah1Δ nem1Δ*.

wild type *PAH1* was accompanied by a 35% increase in phospholipids (Fig. 11B) (29). These observations further emphasized the importance of Nem1p-Spo7p-mediated dephosphorylation of Pah1p for PAP function *in vivo* (29). In *pah1Δ NEM1* cells, the expression of the PKA phosphorylation site alanine/aspartate mutant alleles had relatively minor effects on the amount of TAG (Fig. 11A). However, the phosphorylation site mutations had more dramatic effects on TAG content when they were expressed in *pah1Δ nem1Δ* cells (Fig. 11A). The S10A mutation caused a 57% increase in TAG content, whereas the S10D mutation caused a 37% decrease in TAG, and the difference in TAG between the S10A and S10D mutations was 2.5-fold. The effects of the 5A and 5D mutations on TAG content mirrored the effects of the S10A and S10D mutations, respectively, and the 4A and 4D mutations were not distinguished from the wild type control (data not shown). Thus, of the five PKA sites, the phosphorylation state of Ser-10 played the major role in regulating PAP function. In combination with the 7A mutations, S10A caused a 347% increase in TAG content when compared with the wild type control (Fig. 11A). As described previously (29, 32), the 7A mutations caused a 244% increase in TAG content, and the S10D mutation attenuated this effect by 20% (Fig. 11A). The difference in the amount of TAG between the S10A + 7A and S10D + 7A mutations was 1.6-fold. Although the effects of the phosphorylation site mutations on the total phospholipid content were not great, there were correlations between the relative amounts of TAG and phospholipids of *pah1Δ nem1Δ* cells expressing the S10A and S10D mutations (Fig. 11B).

DISCUSSION

Pah1p PAP in yeast plays a crucial role in lipid homeostasis by controlling the relative proportions of its substrate PA and its product DAG (9, 24). The imbalance of these lipid intermediates due to a defect in PAP activity results in a variety of cellular dysfunctions that include the misregulation of lipid synthesis, an abnormal expansion of the nuclear/ER membrane, defects in lipid droplet formation and vacuole fragmentation, and acute sensitivity to fatty acid-induced toxicity (9, 23–27). Phosphorylation/dephosphorylation of Pah1p has emerged as a major mechanism by which its PAP activity is regulated in yeast. Phosphorylation is associated with the inhibition of PAP, whereas dephosphorylation is associated with its stimulation (28, 29, 32). The stimulatory effect of dephosphorylation can be attributed to an increase in Pah1p PAP catalytic activity and to the translocation of the enzyme from the cytosol to the membrane where its substrate PA resides (9, 28, 29, 32). Whereas the dephosphorylation of Pah1p is mediated by only one protein phosphatase (*i.e.* Nem1p-Spo7p complex), its phosphorylation is mediated by multiple protein kinases (28, 29, 32, 33, 41).

Pah1p is a target for Pho85p-Pho80p, Cdc28p-cyclin B, Dbf2p-Mob1p, PKA, protein kinase C, and casein kinase II (25, 32, 35–37, 41, 71, 74). In this work, we advanced the understanding of this complex regulation by characterizing the phosphorylation by PKA, identifying the sites of phosphorylation, and determining its biochemical and physiological relevance. Moreover, this work established that the phosphorylation by PKA functioned in conjunction with the phosphorylations of Pah1p by Pho85p-Pho80p and Cdc28p-cyclin B.

PKA utilized Pah1p as a substrate with high specificity having K_m values for Pah1p and ATP within the micromolar range previously found for the phosphorylations by Pho85p-Pho80p and Cdc28p-cyclin B (29, 32). The phosphorylation by PKA caused a decrease in PAP catalytic efficiency as reflected in a decrease in V_{max} and an increase in K_m values for PA. In addition, the phosphorylation by PKA causes a decrease in Pah1p interaction with PC-PA liposome membranes (41), supporting a negative regulatory role for the phosphorylation. We identified five sites of phosphorylation as follows: one site (*i.e.* Ser-10) was found within the amphipathic helix at the N terminus of Pah1p, and the remaining sites were located at the C terminus of the protein (Fig. 1). Considering that five sites were targets of PKA, the stoichiometry of phosphorylation was only 1 mol of phosphate/mol of Pah1p. One explanation for this is that not all sites were phosphorylated to the same extent. For example, the phosphopeptide mapping experiments indicated that Ser-677 and Ser-773 were the most heavily phosphorylated sites when compared with the other sites. Another explanation might be that phosphorylation of one site inhibited the phosphorylation of another site (75). The simultaneous mutations of the five sites to alanine (*e.g.* 5A mutations) eliminated the PKA-mediated phosphorylation of Pah1p and the inhibition of PAP activity. Although Ser-10 was not the most heavily phosphorylated site, its phosphorylation inhibited membrane association, PAP activity, and TAG synthesis. Ironically, the phosphorylation of Ser-10 stabilized Pah1p abundance. None of the other single

site mutations affected these properties, but their phosphorylations might be a mechanism by which the phosphorylation and function of Ser-10 or other sites might be controlled. Whether the phosphorylation of Ser-10 specifically affected the function of the amphipathic helix will require additional studies.

Of the protein kinases known to phosphorylate Pah1p, Pho85p-Pho80p has the greatest effect on PAP function (32, 71). The phosphorylation by this complex inhibits PAP activity, location, and function in lipid synthesis, as well as stabilizing enzyme abundance (32). Cdc28p-cyclin B phosphorylates three of the sites phosphorylated by Pho85p-Pho80p (Fig. 1), but the phosphorylation of the three individual sites does not impart much regulation (71). The phosphorylation of Pah1p by PKA at Ser-10 had similar effects on PAP regulation as that of Pho85p-Pho80p, but the extent of the PKA-mediated regulation was not as great. However, in combination with the 7A mutations, the S10A and S10D mutations had greater effects. On the one hand, the S10A mutation enhanced the regulatory effects that the 7A mutations have on enzyme abundance, localization, and role in TAG synthesis. In fact, the enhanced effects of S10A on PAP function resulted in a slow growth phenotype during the exponential phase. This phenotype could be complemented by supplementations of inositol and choline indicating that increased PAP function with respect to TAG synthesis was detrimental to membrane phospholipid synthesis. A similar phenomenon has been described for cells that massively overexpress (*GAL1/10*-directed expression of a high copy number plasmid) the 7A mutations (28, 71). However, in the present work, increased PAP function was governed by low copy expression of S10A + 7A, emphasizing the importance of the PKA-mediated phosphorylation at Ser-10. On the other hand, the S10D mutation attenuated the positive effects 7A mutations have on Pah1p association with membranes and on the synthesis of TAG. S10D also reversed the destabilizing effect that the 7A mutations have on Pah1p abundance. It was also noteworthy that S10D mutation alone caused a loss of growth at 37 °C when the mutant enzyme was expressed in the *nem1Δ* mutant background. Collectively, these data indicated that the PKA-mediated phosphorylation of Ser-10 functions in conjunction with the phosphorylations mediated by Pho85p-Pho80p and Cdc28p-cyclin B and that phospho-Ser-10 should be dephosphorylated for proper PAP function. The paradoxical effects of phosphorylation/dephosphorylation on Pah1p abundance/function appear to be an additional mechanism by which cells control the levels of PA and DAG to maintain lipid homeostasis.

PKA activity is associated with rapid cell growth, enhanced metabolic activity, and an increase in membrane phospholipid synthesis (42–44). With respect to phospholipid synthesis, PKA phosphorylates and has positive effects on the activities/functions of Cho1p phosphatidylserine synthase (60, 76), Ura7p CTP synthetase (65, 77, 78), and Cki1p choline kinase (66, 79). The former and latter enzymes catalyze the committed steps in the synthesis of PC (most abundant phospholipid) via the CDP-DAG and Kennedy pathways, respectively (44, 73). The essential CTP synthetase enzyme (80) provides the CTP required for PC synthesis via both biosynthetic pathways (44, 73). In the exponential phase of growth, the synthesis of phospholipids

Phosphorylation of Yeast Phosphatidate Phosphatase

occurs at the expense of TAG (81). Thus, the PKA-mediated stimulation of these phospholipid biosynthetic activities coupled to the PKA-mediated inhibition of Pah1p PAP coordinates lipid synthesis during growth.

There are checks and balances in lipid metabolism whereby a biochemical form of regulation is counterbalanced by a transcriptional form of regulation (44, 73). The PKA-mediated phosphorylation of Pah1p and that of the transcriptional repressor Opi1p (67) appear to be components of this form of regulation. Opi1p is tethered to the nuclear/ER membrane through interactions with Scs2p and PA (82, 83). These interactions are destabilized when PA levels are reduced, a consequence that causes the translocation of Opi1p from the nuclear/ER membrane into the nucleus where it binds to Ino2p and attenuates the transcriptional activation of UAS_{INO}-containing genes by the Ino2p-Ino4p complex (44, 72, 73, 83). Pah1p PAP activity regulates PA levels and the transcriptional regulation of phospholipid synthesis gene expression. For example, loss of PAP activity and the elevation of PA content result in the derepression of UAS_{INO}-containing genes (23, 25, 28). *CHO1* (encoding phosphatidylserine synthase) and *CKII* (encoding choline kinase) are UAS_{INO}-containing genes (73). Although the PKA-mediated phosphorylation of Pah1p inhibits PAP activity for elevated PA content, the phosphorylation of Opi1p at Ser-31 and Ser-251 by PKA stimulates its repressor activity (67). How PKA stimulates Opi1p function is unknown, but the introduction of negative charges to Opi1p might destabilize its interaction with PA and/or Scs2p at the nuclear/ER membrane. Nonetheless, the PKA-mediated phosphorylations of Pah1p and Opi1p could work together in balancing lipid synthesis from the PA node in the pathways.

Acknowledgments—We acknowledge Florencia Pascual for the critical reading of the manuscript. We also thank Symeon Siniossoglou for supplying the *pah1Δ* and *pah1Δ nem1Δ* mutants and the Pah1p purified from yeast. The mass spectrometry data were obtained from a Orbitrap instrument funded in part by National Institutes of Health Grant NS046593 for the support of the University of Medicine and Dentistry of New Jersey Neuroproteomics Core Facility.

REFERENCES

1. Smith, S. W., Weiss, S. B., and Kennedy, E. P. (1957) The enzymatic dephosphorylation of phosphatidic acids. *J. Biol. Chem.* **228**, 915–922
2. Reue, K., and Brindley, D. N. (2008) Multiple roles for lipins/phosphatidate phosphatase enzymes in lipid metabolism. *J. Lipid Res.* **49**, 2493–2503
3. Reue, K., and Dwyer, J. R. (2009) Lipin proteins and metabolic homeostasis. *J. Lipid Res.* **50**, S109–S114
4. Carman, G. M., and Han, G. S. (2009) Phosphatidic acid phosphatase, a key enzyme in the regulation of lipid synthesis. *J. Biol. Chem.* **284**, 2593–2597
5. Csaki, L. S., and Reue, K. (2010) Lipins. Multifunctional lipid metabolism proteins. *Annu. Rev. Nutr.* **30**, 257–272
6. Brindley, D. N. (1984) Intracellular translocation of phosphatidate phosphohydrolase and its possible role in the control of glycerolipid synthesis. *Prog. Lipid Res.* **23**, 115–133
7. Carman, G. M., and Han, G. S. (2006) Roles of phosphatidate phosphatase enzymes in lipid metabolism. *Trends Biochem. Sci.* **31**, 694–699
8. Brindley, D. N., Pilquill, C., Sariahmetoglu, M., and Reue, K. (2009) Phosphatidate degradation. Phosphatidate phosphatases (lipins) and lipid phosphate phosphatases. *Biochim. Biophys. Acta* **1791**, 956–961
9. Han, G. S., Wu, W. I., and Carman, G. M. (2006) The *Saccharomyces cerevisiae* lipin homolog is a Mg²⁺-dependent phosphatidate phosphatase enzyme. *J. Biol. Chem.* **281**, 9210–9218
10. Lin, Y. P., and Carman, G. M. (1989) Purification and characterization of phosphatidate phosphatase from *Saccharomyces cerevisiae*. *J. Biol. Chem.* **264**, 8641–8645
11. Lin, Y. P., and Carman, G. M. (1990) Kinetic analysis of yeast phosphatidate phosphatase toward Triton X-100/phosphatidate mixed micelles. *J. Biol. Chem.* **265**, 166–170
12. Wu, W. I., Lin, Y. P., Wang, E., Merrill, A. H., Jr., and Carman, G. M. (1993) Regulation of phosphatidate phosphatase activity from the yeast *Saccharomyces cerevisiae* by sphingoid bases. *J. Biol. Chem.* **268**, 13830–13837
13. Wu, W. I., and Carman, G. M. (1994) Regulation of phosphatidate phosphatase activity from the yeast *Saccharomyces cerevisiae* by nucleotides. *J. Biol. Chem.* **269**, 29495–29501
14. Wu, W. I., and Carman, G. M. (1996) Regulation of phosphatidate phosphatase activity from the yeast *Saccharomyces cerevisiae* by phospholipids. *Biochemistry* **35**, 3790–3796
15. Han, G. S., and Carman, G. M. (2010) Characterization of the human *LPIN1*-encoded phosphatidate phosphatase isoforms. *J. Biol. Chem.* **285**, 14628–14638
16. Péterfy, M., Phan, J., Xu, P., and Reue, K. (2001) Lipodystrophy in the *fld* mouse results from mutation of a new gene encoding a nuclear protein, lipin. *Nat. Genet.* **27**, 121–124
17. Donkor, J., Sariahmetoglu, M., Dewald, J., Brindley, D. N., and Reue, K. (2007) Three mammalian lipins act as phosphatidate phosphatases with distinct tissue expression patterns. *J. Biol. Chem.* **282**, 3450–3457
18. Valente, V., Maia, R. M., Vianna, M. C., and Paçó-Larson, M. L. (2010) *Drosophila melanogaster* lipins are tissue-regulated and developmentally regulated and present specific subcellular distributions. *FEBS J.* **277**, 4775–4788
19. Ugrankar, R., Liu, Y., Provaznik, J., Schmitt, S., and Lehmann, M. (2011) Lipin is a central regulator of adipose tissue development and function in *Drosophila*. *Mol. Cell. Biol.* **31**, 1646–1656
20. Golden, A., Liu, J., and Cohen-Fix, O. (2009) Inactivation of the *C. elegans* lipin homolog leads to ER disorganization and to defects in the breakdown and reassembly of the nuclear envelope. *J. Cell Sci.* **122**, 1970–1978
21. Nakamura, Y., Koizumi, R., Shui, G., Shimojima, M., Wenk, M. R., Ito, T., and Ohta, H. (2009) *Arabidopsis* lipins mediate eukaryotic pathway of lipid metabolism and cope critically with phosphate starvation. *Proc. Natl. Acad. Sci. U.S.A.* **106**, 20978–20983
22. Eastmond, P. J., Quettier, A. L., Kroon, J. T., Craddock, C., Adams, N., and Slabas, A. R. (2010) Phosphatidic acid phosphohydrolase 1 and 2 regulate phospholipid synthesis at the endoplasmic reticulum in *Arabidopsis*. *Plant Cell* **22**, 2796–2811
23. Han, G. S., Siniossoglou, S., and Carman, G. M. (2007) The cellular functions of the yeast lipin homolog Pah1p are dependent on its phosphatidate phosphatase activity. *J. Biol. Chem.* **282**, 37026–37035
24. Fakas, S., Qiu, Y., Dixon, J. L., Han, G. S., Ruggles, K. V., Garbarino, J., Sturley, S. L., and Carman, G. M. (2011) Phosphatidate phosphatase activity plays a key role in protection against fatty acid-induced toxicity in yeast. *J. Biol. Chem.* **286**, 29074–29085
25. Santos-Rosa, H., Leung, J., Grimsey, N., Peak-Chew, S., and Siniossoglou, S. (2005) The yeast lipin Smp2p couples phospholipid biosynthesis to nuclear membrane growth. *EMBO J.* **24**, 1931–1941
26. Adeyo, O., Horn, P. J., Lee, S., Binns, D. D., Chandrabhas, A., Chapman, K. D., and Goodman, J. M. (2011) The yeast lipin orthologue Pah1p is important for biogenesis of lipid droplets. *J. Cell Biol.* **192**, 1043–1055
27. Sasser, T., Qiu, Q. S., Karunakaran, S., Padolina, M., Reyes, A., Flood, B., Smith, S., Gonzales, C., and Fratti, R. A. (2012) The yeast lipin 1 orthologue Pah1p regulates vacuole homeostasis and membrane fusion. *J. Biol. Chem.* **287**, 2221–2236
28. O'Hara, L., Han, G. S., Peak-Chew, S., Grimsey, N., Carman, G. M., and Siniossoglou, S. (2006) Control of phospholipid synthesis by phosphorylation of the yeast lipin Pah1p/Smp2p Mg²⁺-dependent phosphatidate phosphatase. *J. Biol. Chem.* **281**, 34537–34548
29. Choi, H. S., Su, W. M., Morgan, J. M., Han, G. S., Xu, Z., Karanasios, E.,

- Siniossoglou, S., and Carman, G. M. (2011) Phosphorylation of phosphatidate phosphatase regulates its membrane association and physiological functions in *Saccharomyces cerevisiae*. Identification of Ser⁶⁰², Thr⁷²³, and Ser⁷⁴⁴ as the sites phosphorylated by CDC28 (CDK1)-encoded cyclin-dependent kinase. *J. Biol. Chem.* **286**, 1486–1498
30. Fakas, S., Konstantinou, C., and Carman, G. M. (2011) *DGK1*-encoded diacylglycerol kinase activity is required for phospholipid synthesis during growth resumption from stationary phase in *Saccharomyces cerevisiae*. *J. Biol. Chem.* **286**, 1464–1474
31. Karanasios, E., Han, G. S., Xu, Z., Carman, G. M., and Siniossoglou, S. (2010) A phosphorylation-regulated amphipathic helix controls the membrane translocation and function of the yeast phosphatidate phosphatase. *Proc. Natl. Acad. Sci. U.S.A.* **107**, 17539–17544
32. Choi, H. S., Su, W. M., Han, G. S., Plote, D., Xu, Z., and Carman, G. M. (2012) Pho85p-Pho80p phosphorylation of yeast Pah1p phosphatidate phosphatase regulates its activity, location, abundance, and function in lipid metabolism. *J. Biol. Chem.* **287**, 11290–11301
33. Siniossoglou, S., Santos-Rosa, H., Rappsilber, J., Mann, M., and Hurt, E. (1998) A novel complex of membrane proteins required for formation of a spherical nucleus. *EMBO J.* **17**, 6449–6464
34. Blom, N., Sicheritz-Pontén, T., Gupta, R., Gammeltoft, S., and Brunak, S. (2004) Prediction of post-translational glycosylation and phosphorylation of proteins from the amino acid sequence. *Proteomics* **4**, 1633–1649
35. Ptacek, J., Devgan, G., Michaud, G., Zhu, H., Zhu, X., Fasolo, J., Guo, H., Jona, G., Breitkreutz, A., Sopko, R., McCartney, R. R., Schmidt, M. C., Rachidi, N., Lee, S. J., Mah, A. S., Meng, L., Stark, M. J., Stern, D. F., De Virgilio, C., Tyers, M., Andrews, B., Gerstein, M., Schweitzer, B., Predki, P. F., and Snyder, M. (2005) Global analysis of protein phosphorylation in yeast. *Nature* **438**, 679–684
36. Dephoure, N., Howson, R. W., Blethrow, J. D., Shokat, K. M., and O'Shea, E. K. (2005) Combining chemical genetics and proteomics to identify protein kinase substrates. *Proc. Natl. Acad. Sci. U.S.A.* **102**, 17940–17945
37. Ubersax, J. A., Woodbury, E. L., Quang, P. N., Paraz, M., Blethrow, J. D., Shah, K., Shokat, K. M., and Morgan, D. O. (2003) Targets of the cyclin-dependent kinase Cdk1. *Nature* **425**, 859–864
38. Enserink, J. M., and Kolodner, R. D. (2010) An overview of Cdk1-controlled targets and processes. *Cell Div.* **5**, 11
39. Moffat, J., Huang, D., and Andrews, B. (2000) Functions of Pho85 cyclin-dependent kinases in budding yeast. *Prog. Cell Cycle Res.* **4**, 97–106
40. Carroll, A. S., and O'Shea, E. K. (2002) Pho85 and signaling environmental conditions. *Trends Biochem. Sci.* **27**, 87–93
41. Xu, Z., Su, W. M., and Carman, G. M. (2012) Fluorescence spectroscopy measures yeast *PAH1*-encoded phosphatidate phosphatase interaction with liposome membranes. *J. Lipid Res.* **53**, 522–528
42. Broach, J. R., and Deschenes, R. J. (1990) The function of RAS genes in *Saccharomyces cerevisiae*. *Adv. Cancer Res.* **54**, 79–139
43. Thevelein, J. M. (1994) Signal transduction in yeast. *Yeast* **10**, 1753–1790
44. Carman, G. M., and Han, G. S. (2011) Regulation of phospholipid synthesis in the yeast *Saccharomyces cerevisiae*. *Annu. Rev. Biochem.* **80**, 859–883
45. Han, G. S., Sreenivas, A., Choi, M. G., Chang, Y. F., Martin, S. S., Baldwin, E. P., and Carman, G. M. (2005) Expression of human CTP synthetase in *Saccharomyces cerevisiae* reveals phosphorylation by protein kinase A. *J. Biol. Chem.* **280**, 38328–38336
46. Rose, M. D., Winston, F., and Heiter, P. (1990) *Methods in Yeast Genetics: A Laboratory Course Manual*, Cold Spring Harbor Laboratory Press, Cold Spring Harbor, NY
47. Culbertson, M. R., and Henry, S. A. (1975) Inositol requiring mutants of *Saccharomyces cerevisiae*. *Genetics* **80**, 23–40
48. Zwietering, M. H., Jongenburger, I., Rombouts, F. M., and van't Riet, K. (1990) Modeling of the bacterial growth curve. *Appl. Environ. Microbiol.* **56**, 1875–1881
49. Sambrook, J., Fritsch, E. F., and Maniatis, T. (1989) *Molecular Cloning: A Laboratory Manual*, 2nd Ed., Cold Spring Harbor Laboratory, Cold Spring Harbor, NY
50. Innis, M. A., and Gelfand, D. H. (1990) in *PCR Protocols. A Guide to Methods and Applications* (Innis, M. A., Gelfand, D. H., Sninsky, J. J., and White, T. J., eds) pp. 3–12, Academic Press, Inc., San Diego
51. Ito, H., Fukuda, Y., Murata, K., and Kimura, A. (1983) Transformation of intact yeast cells treated with alkali cations. *J. Bacteriol.* **153**, 163–168
52. Carman, G. M., and Lin, Y. P. (1991) Phosphatidate phosphatase from yeast. *Methods Enzymol.* **197**, 548–553
53. Bradford, M. M. (1976) A rapid and sensitive method for the quantitation of microgram quantities of protein utilizing the principle of protein-dye binding. *Anal. Biochem.* **72**, 248–254
54. Laemmli, U. K. (1970) Cleavage of structural proteins during the assembly of the head of bacteriophage T4. *Nature* **227**, 680–685
55. Boyle, W. J., van der Geer, P., and Hunter, T. (1991) Phosphopeptide mapping and phosphoamino acid analysis by two-dimensional separation on thin-layer cellulose plates. *Methods Enzymol.* **201**, 110–149
56. Yang, W. L., and Carman, G. M. (1995) Phosphorylation of CTP synthetase from *Saccharomyces cerevisiae* by protein kinase C. *J. Biol. Chem.* **270**, 14983–14988
57. MacDonald, J. I., and Kent, C. (1994) Identification of phosphorylation sites in rat liver CTP:phosphocholine cytidylyltransferase. *J. Biol. Chem.* **269**, 10529–10537
58. Burnette, W. (1981) Western blotting. Electrophoretic transfer of proteins from sodium dodecyl sulfate-polyacrylamide gels to unmodified nitrocellulose and radiographic detection with antibody and radioiodinated protein A. *Anal. Biochem.* **112**, 195–203
59. Haid, A., and Suissa, M. (1983) Immunochemical identification of membrane proteins after sodium dodecyl sulfate-polyacrylamide gel electrophoresis. *Methods Enzymol.* **96**, 192–205
60. Choi, H. S., Han, G. S., and Carman, G. M. (2010) Phosphorylation of yeast phosphatidylserine synthase by protein kinase A. Identification of Ser⁴⁶ and Ser⁴⁷ as major sites of phosphorylation. *J. Biol. Chem.* **285**, 11526–11536
61. Morlock, K. R., Lin, Y. P., and Carman, G. M. (1988) Regulation of phosphatidate phosphatase activity by inositol in *Saccharomyces cerevisiae*. *J. Bacteriol.* **170**, 3561–3566
62. Bligh, E. G., and Dyer, W. J. (1959) A rapid method of total lipid extraction and purification. *Can. J. Biochem. Physiol.* **37**, 911–917
63. Henderson, R. J., and Tocher, D. R. (1992) in *Lipid Analysis* (Hamilton, R. J., and Hamilton, S., eds) pp. 65–111, IRL Press, New York
64. Toda, T., Cameron, S., Sass, P., Zoller, M., and Wigler, M. (1987) Three different genes in *S. cerevisiae* encode the catalytic subunits of the cAMP-dependent protein kinase. *Cell* **50**, 277–287
65. Yang, W. L., and Carman, G. M. (1996) Phosphorylation and regulation of CTP synthetase from *Saccharomyces cerevisiae* by protein kinase A. *J. Biol. Chem.* **271**, 28777–28783
66. Kim, K. H., and Carman, G. M. (1999) Phosphorylation and regulation of choline kinase from *Saccharomyces cerevisiae* by protein kinase A. *J. Biol. Chem.* **274**, 9531–9538
67. Sreenivas, A., and Carman, G. M. (2003) Phosphorylation of the yeast phospholipid synthesis regulatory protein *Opilp* by protein kinase A. *J. Biol. Chem.* **278**, 20673–20680
68. Krebs, E. G., and Beavo, J. A. (1979) Phosphorylation-dephosphorylation of enzymes. *Annu. Rev. Biochem.* **48**, 923–959
69. Carman, G. M., Deems, R. A., and Dennis, E. A. (1995) Lipid signaling enzymes and surface dilution kinetics. *J. Biol. Chem.* **270**, 18711–18714
70. Han, G. S., and Carman, G. M. (2004) Assaying lipid phosphate phosphatase activities. *Methods Mol. Biol.* **284**, 209–216
71. Kastaniotis, A. J., Autio, K. J., Sormunen, R. T., and Hiltunen, J. K. (2004) Htd2p/Yhr067p is a yeast 3-hydroxyacyl-ACP dehydratase essential for mitochondrial function and morphology. *Mol. Microbiol.* **53**, 1407–1421
72. Carman, G. M., and Henry, S. A. (2007) Phosphatidic acid plays a central role in the transcriptional regulation of glycerophospholipid synthesis in *Saccharomyces cerevisiae*. *J. Biol. Chem.* **282**, 37293–37297
73. Henry, S. A., Kohlwein, S. D., and Carman, G. M. (2012) Metabolism and regulation of glycerolipids in the yeast *Saccharomyces cerevisiae*. *Genetics* **190**, 317–349
74. Mah, A. S., Elia, A. E., Devgan, G., Ptacek, J., Schutkowski, M., Snyder, M., Yaffe, M. B., and Deshaies, R. J. (2005) Substrate specificity analysis of protein kinase complex Dbf2-Mob1 by peptide library and proteome array screening. *BMC Biochem.* **6**, 22
75. Roach, P. J. (1991) Multisite and hierarchal protein phosphorylation.

Phosphorylation of Yeast Phosphatidate Phosphatase

- J. Biol. Chem.* **266**, 14139–14142
76. Kinney, A. J., and Carman, G. M. (1988) Phosphorylation of yeast phosphatidylserine synthase *in vivo* and *in vitro* by cyclic AMP-dependent protein kinase. *Proc. Natl. Acad. Sci. U.S.A.* **85**, 7962–7966
77. Park, T. S., Ostrander, D. B., Pappas, A., and Carman, G. M. (1999) Identification of Ser⁴²⁴ as the protein kinase A phosphorylation site in CTP synthetase from *Saccharomyces cerevisiae*. *Biochemistry* **38**, 8839–8848
78. Choi, M. G., Park, T. S., and Carman, G. M. (2003) Phosphorylation of *Saccharomyces cerevisiae* CTP synthetase at Ser⁴²⁴ by protein kinases A and C regulates phosphatidylcholine synthesis by the CDP-choline pathway. *J. Biol. Chem.* **278**, 23610–23616
79. Yu, Y., Sreenivas, A., Ostrander, D. B., and Carman, G. M. (2002) Phosphorylation of *Saccharomyces cerevisiae* choline kinase on Ser³⁰ and Ser⁸⁵ by protein kinase A regulates phosphatidylcholine synthesis by the CDP-choline pathway. *J. Biol. Chem.* **277**, 34978–34986
80. Ozier-Kalogeropoulos, O., Adeline, M. T., Yang, W. L., Carman, G. M., and Lacroute, F. (1994) Use of synthetic lethal mutants to clone and characterize a novel CTP synthetase gene in *Saccharomyces cerevisiae*. *Mol. Gen. Genet.* **242**, 431–439
81. Taylor, F. R., and Parks, L. W. (1979) Triacylglycerol metabolism in *Saccharomyces cerevisiae* relation to phospholipid synthesis. *Biochim. Biophys. Acta* **575**, 204–214
82. Loewen, C. J., Roy, A., and Levine, T. P. (2003) A conserved ER targeting motif in three families of lipid-binding proteins and in Opi1p binds VAP. *EMBO J.* **22**, 2025–2035
83. Loewen, C. J., Gaspar, M. L., Jesch, S. A., Delon, C., Ktistakis, N. T., Henry, S. A., and Levine, T. P. (2004) Phospholipid metabolism regulated by a transcription factor sensing phosphatidic acid. *Science* **304**, 1644–1647
84. Han, G. S., O'Hara, L., Carman, G. M., and Siniosoglou, S. (2008) An unconventional diacylglycerol kinase that regulates phospholipid synthesis and nuclear membrane growth. *J. Biol. Chem.* **283**, 20433–20442
85. Sikorski, R. S., and Hieter, P. (1989) A system of shuttle vectors and yeast host strains designed for efficient manipulation of DNA in *Saccharomyces cerevisiae*. *Genetics* **122**, 19–27